

The rise of 2D dielectrics/ferroelectrics F

Cite as: APL Mater. 7, 120902 (2019); <https://doi.org/10.1063/1.5129447>

Submitted: 28 September 2019 • Accepted: 17 November 2019 • Published Online: 09 December 2019

 Minoru Osada and  Takayoshi Sasaki

COLLECTIONS

 This paper was selected as Featured



View Online



Export Citation



CrossMark

ARTICLES YOU MAY BE INTERESTED IN

[Ferroelectric thin films: Review of materials, properties, and applications](#)

Journal of Applied Physics **100**, 051606 (2006); <https://doi.org/10.1063/1.2336999>

[Ferroelectric field effect transistors: Progress and perspective](#)

APL Materials **9**, 021102 (2021); <https://doi.org/10.1063/5.0035515>

[Ferroelectric or non-ferroelectric: Why so many materials exhibit “ferroelectricity” on the nanoscale](#)

Applied Physics Reviews **4**, 021302 (2017); <https://doi.org/10.1063/1.4979015>



APL Materials
Roadmaps

Where is your field headed?

The rise of 2D dielectrics/ferroelectrics

Cite as: APL Mater. 7, 120902 (2019); doi: 10.1063/1.5129447
Submitted: 28 September 2019 • Accepted: 17 November 2019 •
Published Online: 9 December 2019



Minoru Osada^{1,2,a)}  and Takayoshi Sasaki² 

AFFILIATIONS

¹Institute of Materials and Systems for Sustainability (IMaSS), Nagoya University, Nagoya 464-8601, Japan

²International Center for Materials Nanoarchitectonics (WPI-MANA), National Institute for Materials Science (NIMS), Tsukuba, Ibaraki 305-0044, Japan

^{a)} Author to whom correspondence should be addressed: mosada@imass.nagoya-u.ac.jp

ABSTRACT

Ultrathin films with high- k dielectric/ferroelectric properties form the basis of modern electronics. With further miniaturization of electronic devices, conventional materials are expected to experience a challenge because of their critical thickness, where the dielectric/ferroelectric responses are unstable or even disappeared if the film thickness is reduced to the nanometer scale or below a two-dimensional (2D) limit. Owing to the benefit of preparing stable atomically thin film, 2D materials present tantalizing prospects for scaling high- k dielectric/ferroelectric technologies down to the actual atomic scale. Here, we review recent progress in 2D dielectrics/ferroelectrics and related device applications.

© 2019 Author(s). All article content, except where otherwise noted, is licensed under a Creative Commons Attribution (CC BY) license (<http://creativecommons.org/licenses/by/4.0/>). <https://doi.org/10.1063/1.5129447>

I. INTRODUCTION

Ultrathin films with high- k dielectric/ferroelectric properties form the basis of modern electronics such as memories, field-effect transistors (FETs), capacitors, and sensors. For further miniaturization of electronic devices, the exploration of high- k dielectric/ferroelectric thin films with nanometer thicknesses are strongly needed.^{1–3} However, the so-called size effects present a formidable challenge (Fig. 1).^{4–6} Previous studies on high- k dielectric thin films have consistently observed that the dielectric constant (ϵ_r) is significantly reduced as the film thickness decreases to 50 nm.^{7,8} For example, perovskite thin films (such as BaTiO₃ and PbTiO₃) often yield reduced ϵ_r values that are 2–3 orders of magnitude smaller than the bulk values.^{8–11} This problem is even more pronounced in ferroelectric thin films.^{12,13} In conventional ferroelectrics (such as BaTiO₃, PbTiO₃, SrBi₂Ta₂O₉, and Bi₄Ti₃O₁₂),^{14–16} the electric polarization reduces or even disappears when the film thickness reaches the deep nanoscale regime or a critical thickness.^{8–11} This size effect is often discussed in terms of intrinsic size or depolarizing field effects arising in ultrathin dielectrics/ferroelectrics.^{5,17–20} Despite intensive studies, the underlying physics behind the critical thickness and size effects is still debatable because competing effects such as the imperfect charge screening and dead-layer effects (the local chemical environment, defects/strains at the interface, and

electrical boundary conditions) cause complicated behaviors in measured properties.^{4,5,18}

With recent advances in thin-film technologies and nanoscale characterization methods, the understanding of nanoscale ferroelectricity has continued to evolve from early studies indicating the complete suppression of ferroelectricity to recent reports demonstrating the enhancement in local ferroelectricity by strain engineering²¹ or even the possible absence of a critical thickness.²² Current nanoscale characterization techniques, including scanning probe microscopy (SPM) and transmission electron microscopy (TEM), have allowed the detection of ferroelectricity in perovskite films down to a thickness of a few unit cells; ferroelectricity could be retained down to 1.2–4 nm (PbTiO₃),^{13,23} 1.6–3 nm (BaTiO₃),^{24,25} and ~3 nm (BaFeO₃).²⁶ State-of-the-art characterization using high-resolution TEM indicated a possible absence of a critical thickness in ultrathin ferroelectric films; in the PbZr_{0.2}Ti_{0.8}O₃ case, the residual polarization was observed even at 0.8 nm.²² With the integration of high- k dielectrics/ferroelectrics into electronics, this size-effect issue becomes increasingly important since intrinsic size effects may limit the device performance.

Owing to their atomic-scale thickness, 2D nanosheets present a tantalizing prospect for scaling high- k dielectric/ferroelectric technologies down to the actual atomic scale.^{27–29} Since the breakthrough development of graphene,^{30–33} the variety of 2D nanosheets

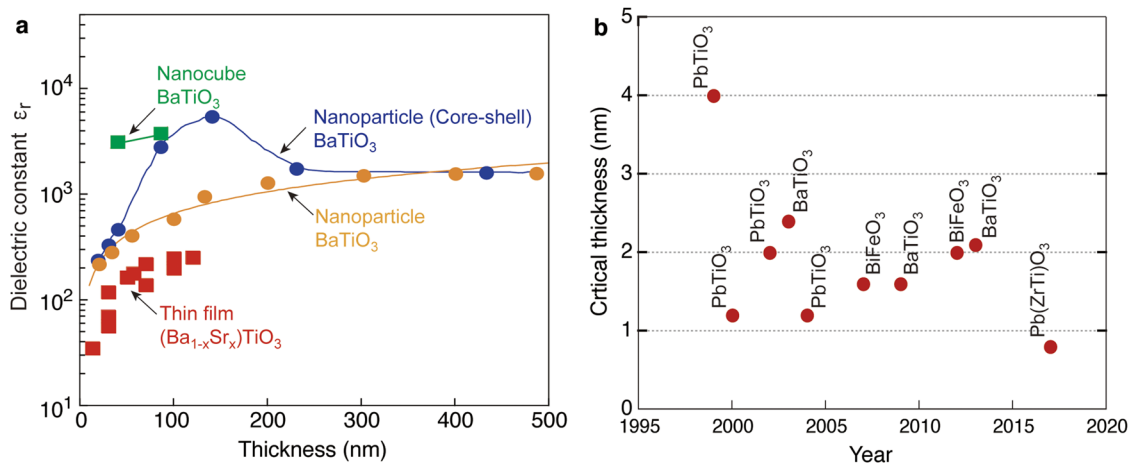


FIG. 1. (a) Size dependence properties of BaTiO₃ nanostructures. (b) Critical thickness for ferroelectricity in perovskite thin films.

has been greatly expanded to inorganic materials including chalcogenides,^{34,35} oxides,^{36,37} MXenes,^{38,39} and black phosphorus.^{40,41} These inorganic nanosheets are very rich in structural diversity and electronic properties such as superconductivity,⁴² valley polarization,⁴³ and quantum magnetism.⁴⁴ Thus, 2D inorganic nanosheets offer a novel platform for exploring emerging phenomena that cannot be realized in graphene. Despite significant advances in graphenelike 2D nanosheets, it remains a challenge to explore their high-*k* dielectric/ferroelectric counterparts, which have great potential in new 2D electronics.⁶ Most 2D nanosheets synthesized so far are conducting or semiconducting with a rather small bandgap²⁸ (Fig. 2), precluding their use in high-*k* dielectric/ferroelectric materials.

2D nanosheets with high polarizability or noncentrosymmetric structures have great potentials for high-*k* dielectrics/ferroelectrics. In particular, 2D oxides possess a wide bandgap (3–4 eV),⁴⁵ which is favorable for realizing high-*k* dielectrics with a highly insulating nature (Fig. 2). In fact, *d*⁰ transition metal oxides (with Ti⁴⁺,

Nb⁵⁺, Ta⁵⁺, and W⁶⁺) can be tailored to yield high-*k* values ($\epsilon_r > 100$).²⁹ To date, two kinds of high-*k* nanosheets have been developed with dielectric constant values above 100. One kind comprises simple oxides^{46,47} with a modest permittivity ($\epsilon_r \sim 100$), e.g., Ti_{1- δ} O₂ and Nb₃O₈; the other comprises perovskites^{48,49} with higher permittivity ($\epsilon_r > 200$). Noncentrosymmetric materials are an important target for 2D ferroelectrics because of spontaneous symmetry breaking and its associated ferroelectric polarization. Recently, a range of 2D nanosheets and/or van der Waals (vdW) materials have been theoretically predicted or experimentally confirmed as ferroelectrics,^{50–52} including transition metal dichalcogenides (e.g., MoS₂, MoTe₂, and WTe₂), group IV monochalcogenides (e.g., SnS, SnSe, GeS, and GeSe), group III–V compounds (e.g., AlSb, GaP, GaAs, and InSb), MXenes (Sc₂CO₂), CuInP₂S₆, and perovskite oxides (Ca₂Na₂Nb₅O₁₆).

From this perspective, we review recent progress in 2D dielectrics/ferroelectrics. We begin with the introduction of 2D dielectrics/ferroelectrics. We also present a perspective on

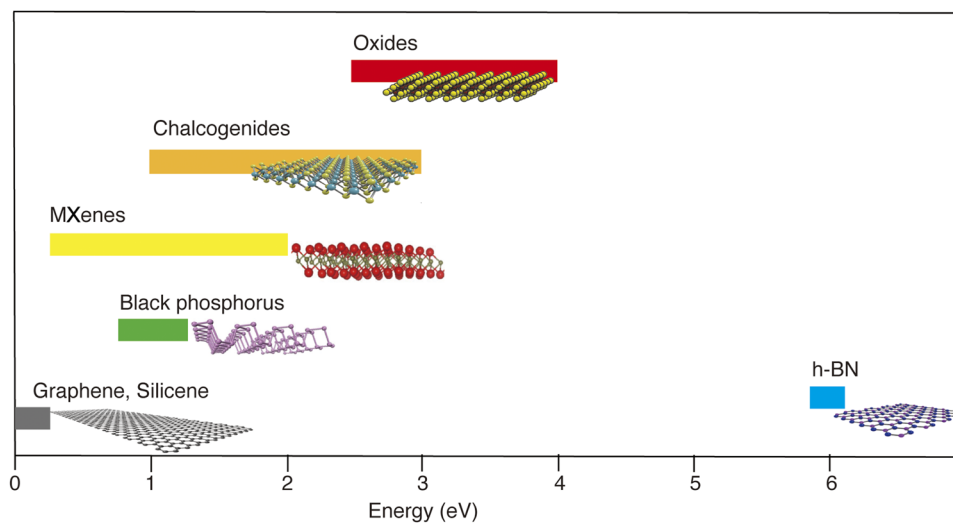


FIG. 2. Bandgap energies for various 2D nanosheets.

the advantages offered by this class of materials for future electronics.

II. 2D DIELECTRICS

2D oxide nanosheets may be the perfect solution as a new era unfolds in 2D dielectrics.⁶ A variety of oxide nanosheets have been synthesized by delaminating layered oxides into their single sheets.^{36,53} Most oxide nanosheets synthesized so far are transition metal oxides comprising d^0 cations (Ti^{4+} , Nb^{5+} , Ta^{5+} , and W^{6+}). Such d^0 oxide nanosheets are wide bandgap semiconductors or insulators and can thus be utilized as high- k dielectrics.

We investigated such possibilities in d^0 oxide nanosheets. Table I summarizes the experimentally confirmed 2D dielectrics. The first experimental realization of 2D dielectrics was a molecularly thin $\text{Ti}_{0.87}\text{O}_2$ nanosheet.⁴⁶ The $\text{Ti}_{0.87}\text{O}_2$ nanosheet is composed of only TiO_6 octahedra, a key building block for Ti-based dielectrics, and can thus be viewed as an ideal basis for high- k dielectrics with a critical thickness [Fig. 3(a)]. Theoretical and experimental investigations revealed a high polarizability in $\text{Ti}_{0.87}\text{O}_2$ nanosheets compared with that of bulk TiO_2 (rutile and anatase), and the multilayer films of $\text{Ti}_{0.87}\text{O}_2$ nanosheets exhibited both a high dielectric constant ($\epsilon_r = 125$) and highly insulating properties ($<10^{-7}$ A/cm²) at thicknesses down to 10 nm.^{46,54} Such a highly insulating nature was attributed to the wide bandgap nature of $\text{Ti}_{0.87}\text{O}_2$ nanosheets. Additionally, $\text{Ti}_{0.87}\text{O}_2$ nanosheets possess Ti vacancies without oxygen vacancies,⁵⁵ which eliminate the well-known problem of high leakage induced by oxygen vacancies. The second family comprises titanoniobate nanosheets (TiNbO_5 , Ti_2NbO_7 , and $\text{Ti}_5\text{NbO}_{14}$) [Fig. 3(a)].⁴⁷ In these nanosheets, site engineering by Nb incorporation promoted the octahedral distortion, resulting in a very high molecular polarizability. The multilayer stacked nanofilms exhibited high ϵ_r values (155–320) with high insulating properties (10^{-6} – 10^{-8} A/cm²) [Fig. 3(b)]. The optimal property was observed in Ti_2NbO_7

[$\text{Nb}/(\text{Ti} + \text{Nb}) = 0.33$], in which ϵ_r reached ~ 320 , the highest value realized to date in simple oxides in the ultrathin region (<30 nm).

Another family of 2D dielectrics is the perovskite nanosheet.^{6,56} Parent layered perovskites form the basis of interesting classes of high- k dielectric/ferroelectric materials including Dion-Jacobson $A' [A_{m-1}B_mO_{3m+1}]$, Ruddlesden-Popper $A'_2[A_{m-1}B_mO_{3m+1}]$, and Aurivillius $[\text{Bi}_2\text{O}_2][A_{m-1}B_mO_{3m+1}]$ (A' = proton, alkali metals, and alkali earth metals, for example; A = lanthanides and Bi; B = Ti, Nb, and Ta; and m = thickness of perovskite slabs). These layered perovskites have very diverse structures and physical properties depending on the A and B cations as well as the number of ABO_3 type perovskite layers (m). They consist of perovskitelike layers incorporated with cations or Bi_2O_2 layers in the interlayer space. Due to their rich chemical reactivity in the interlayer spaces, these compounds have been investigated as important targets for ion-exchange reactions and exfoliated nanosheets. The exfoliation of layered perovskites has been reported for Dion-Jacobson phases^{57–61} [LaNb_2O_7 , $(\text{Ca},\text{Sr})_2(\text{Nb},\text{Ta})_3\text{O}_{10}$, $\text{Ba}_2\text{Ta}_3\text{O}_{10}$, $\text{Ca}_2\text{Ta}_3\text{O}_{10-x}\text{N}_x$, $\text{Ca}_2\text{Na}_{m-3}\text{Nb}_m\text{O}_{3m+1}$ ($m = 4-6$), $\text{CaLaNb}_2\text{TiO}_{10}$, and $\text{La}_2\text{Ti}_2\text{NbO}_{10}$] and for others with Ruddlesden-Popper^{62–64} ($\text{Eu}_{0.56}\text{Ta}_2\text{O}_7$, $\text{SrLaTi}_2\text{TaO}_{10}$, and $\text{Ca}_2\text{Ta}_2\text{TiO}_{10}$) and Aurivillius (Bi_2WO_6 , $\text{SrBi}_2\text{Ta}_2\text{O}_9$, and $\text{Bi}_4\text{Ti}_3\text{O}_{12}$) phases.^{65–67} These nanosheets consist of only a few octahedral units (TiO_6 , NbO_6 , or TaO_6), a key building block for high- k dielectrics/ferroelectrics in perovskites. Perovskite nanosheets can thus be viewed as an ideal basis for high- k dielectric/ferroelectric materials with a critical thickness.

$\text{Ca}_2\text{Nb}_3\text{O}_{10}$ nanosheets have been extensively investigated as high- k dielectrics.^{48,68–71} Layer-by-layer assembly of $\text{Ca}_2\text{Nb}_3\text{O}_{10}$ nanosheets enables engineering of dielectric responses and breakdown voltages to obtain miniaturized capacitors with improved performance. Multilayer stacked nanosheet films exhibited a stable dielectric response ($\epsilon_r = \sim 210$) up to 10 GHz. Moreover, the nanosheet films realized a high capacitance density (~ 20 $\mu\text{F}/\text{cm}^2$),

TABLE I. Summary of the experimentally confirmed 2D dielectrics.

2D materials	ϵ_r	τ (ppm/K)	J (A/cm ²) at +1 V	Breakdown (MV/cm)	References
$\text{Ti}_{0.87}\text{O}_2$	125	+106	3×10^{-8}	3.8	46 and 47
$\text{Ti}_{0.91}\text{O}_2$	90		6×10^{-6}	3.2	46
TiNbO_5	155	−12	9×10^{-9}	3.4	47
Ti_2NbO_7	320	−324	2×10^{-8}	3.4	47
$\text{Ti}_5\text{NbO}_{14}$	300	+5	3×10^{-7}	3.4	47
Nb_3O_8	80	−876	2×10^{-6}	3.0	47
$\text{La}_{0.95}\text{Nb}_2\text{O}_7$	45		3×10^{-6}	2.1	68
$\text{La}_{0.90}\text{Eu}_{0.05}\text{Nb}_2\text{O}_7$	20		8×10^{-6}		68
$\text{Eu}_{0.56}\text{Ta}_2\text{O}_7$	12		6×10^{-7}		68
$\text{Ca}_2\text{Nb}_3\text{O}_{10}$	210	−50	3×10^{-8}	3.4–6.0	48 and 49
$\text{Ca}_2\text{NaNb}_4\text{O}_{13}$	320		3×10^{-9}	3.3	49
$\text{Ca}_2\text{Na}_2\text{Nb}_5\text{O}_{16}$	390		2×10^{-8}	3.2	49
$\text{Ca}_2\text{Na}_3\text{Nb}_6\text{O}_{19}$	470		1×10^{-7}	3.0	49
$\text{Sr}_2\text{Nb}_3\text{O}_{10}$	240	+60	3×10^{-8}	3.2	68
$\text{Ca}_2\text{Ta}_3\text{O}_{10}$	145	−150	6×10^{-9}	3.6	68
$\text{Sr}_2\text{Ta}_3\text{O}_{10}$	175	+80	7×10^{-9}	3.5	68

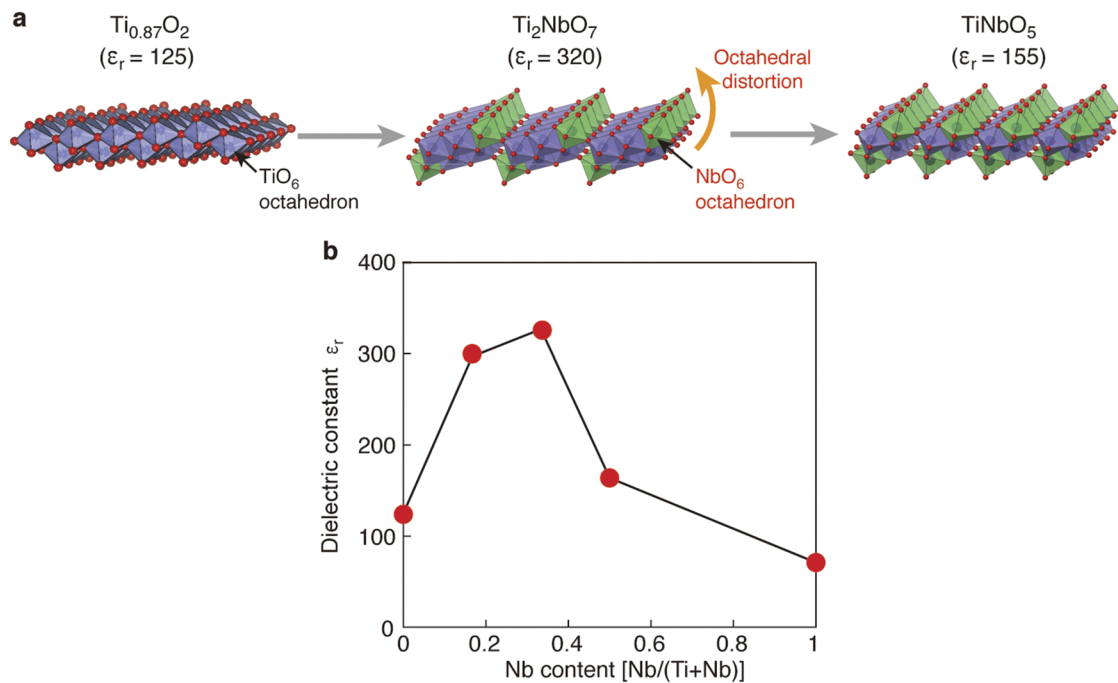


FIG. 3. (a) Structure of Ti-based high- k dielectric nanosheets ($\text{Ti}_{0.87}\text{O}_2$, Ti_2NbO_7 , TiNbO_5). (b) Composition dependence of ϵ_r in multilayer films of $\text{Ti}_{0.87}\text{O}_2$, $\text{Ti}_5\text{NbO}_{14}$, Ti_2NbO_7 , TiNbO_5 , and Nb_3O_8 . Reproduced with permission from Osada *et al.*, *Adv. Funct. Mater.* **21**, 3482 (2011). Copyright 2011 Wiley-VCH Verlag GmbH & Co. KGaA, Weinheim.

insulating properties ($<10^{-7}$ A/cm²), a strong breakdown field (~ 6 MV/cm), and a robust thermal stability up to 250 °C. These excellent dielectric properties of $\text{Ca}_2\text{Nb}_3\text{O}_{10}$ nanosheets offer a new solution for capacitor dielectrics.

Recent research on perovskite nanosheets is directed toward material design by tailoring the composition and structure and improving their high- k performance. In bulk perovskites, a variety of strategies have been utilized for designing new high- k dielectrics,

either by doping more polarizable ions into the lattice or tuning the structural distortion. Such a material design has been achieved in perovskite nanosheets. In $(\text{Ca}_{1-x}\text{Sr}_x)_2(\text{Nb}_{1-y}\text{Ta}_y)_3\text{O}_{10}$ nanosheets, for example, *A*-site modification with Sr^{2+} ions increased the ϵ_r value, whereas *B*-site modification with Ta^{5+} ions improved the insulating characteristics with enlarged bandgap and breakdown voltage.^{6,68} Even elegant engineering was found in 2D homologous perovskite nanosheets ($\text{Ca}_2\text{Na}_{m-3}\text{Nb}_m\text{O}_{3m+1}$; $m = 3-6$) (Fig. 4).⁴⁹

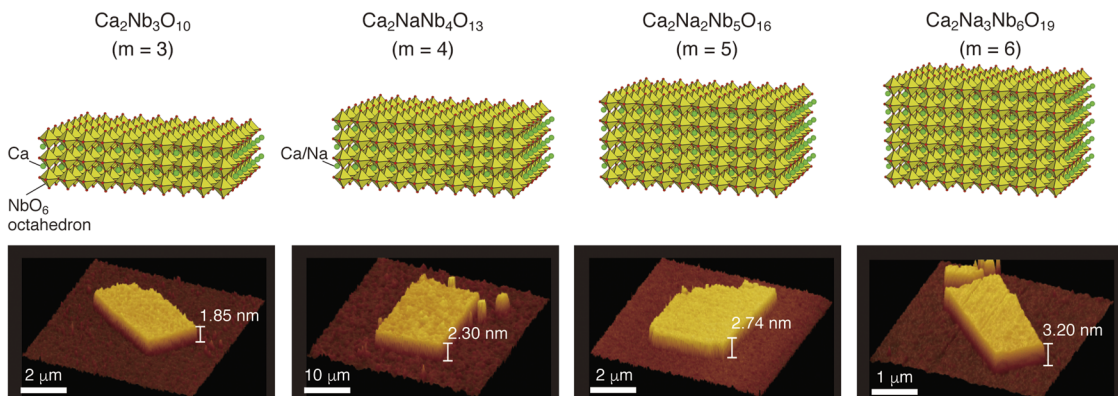


FIG. 4. Structures and AFM images of $\text{Ca}_2\text{Na}_{m-3}\text{Nb}_m\text{O}_{3m+1}$ nanosheets. The thicknesses were approximately 1.9, 2.3, 2.7, and 3.2 nm for $m = 3, 4, 5$, and 6, respectively. The increment of ~ 0.4 nm corresponds to the thickness of one NbO_6 octahedron, which is consistent with the homologous structural aspect of layered perovskites. Reproduced with permission from Li *et al.*, *J. Am. Chem. Soc.* **139**, 10868 (2017). Copyright 2017 American Chemical Society.

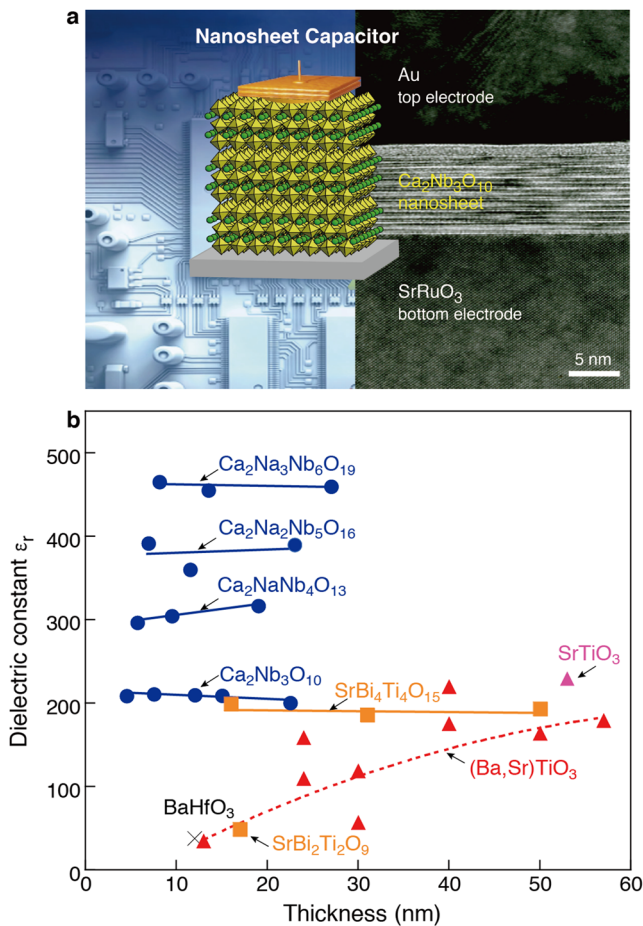


FIG. 5. (a) Schematic illustration and cross-sectional TEM image for a nanocapacitor of perovskite nanosheets. (b) Maximum values of the dielectric constant (ϵ_r) for $\text{Ca}_2\text{Na}_{m-3}\text{Nb}_m\text{O}_{3m+1}$ nanosheets and various perovskite thin films. Reproduced with permission from Li *et al.*, *J. Am. Chem. Soc.* **139**, 10868 (2017). Copyright 2017 American Chemical Society.

In $\text{Ca}_2\text{Na}_{m-3}\text{Nb}_m\text{O}_{3m+1}$, the thickness of perovskite layers can be incrementally controlled by changing m , and such a unit-cell-level engineering enhanced the high- k dielectric response. The $m = 6$ member ($\text{Ca}_2\text{Na}_3\text{Nb}_6\text{O}_{19}$) attained a high dielectric constant of ~ 470 , which is the highest among all known perovskite dielectrics in the ultrathin region (< 10 nm) (Fig. 5). Importantly, the high ϵ_r values of perovskite nanosheets persist even in the < 10 nm region, which is in contrast to the size-induced degradation observed in typical perovskite dielectrics. The unique features of 2D nanosheets make them important and fascinating research targets for ultrascaled high-density capacitors and new energy storage devices.

III. 2D FERROELECTRICS

The existence of 2D ferroelectricity was theoretically predicted long ago. However, there have been a limited number of reports on 2D ferroelectricity until recently since realistic materials suffer from

the fundamental constraint of size effects. In addition, the dead-layer effects due to interfacial strain and local chemical environment can deteriorate ferroelectricity in ultrathin films. In contrast, 2D layered or vdW materials have strong in-plane bonds but weak coupling between the layers, and thus exfoliated 2D nanosheets could provide a pathway to realize 2D ferroelectricity while eliminating the so-called “dead-layer” issues. In recent years, several 2D ferroelectric candidates have been theoretically predicated and experimentally verified (Fig. 6).

Early studies were devoted to theoretical investigations. In principle, 2D nanosheets allow the exploration of ferroelectricity in both the in-plane and out-of-plane directions. In 2014, intrinsic 2D ferroelectricity with out-of-plane (vertical) polarizations was theoretically predicted in 1T MoS_2 monolayers. Using the Landau theoretical analysis with first-principles calculations, Shirodkar and Waghmare demonstrated spontaneous symmetry breaking even in 1T MoS_2 monolayers. Even in the metallic state, 1T MoS_2 induced both bandgap opening and robust ferroelectricity with ordering of electric dipoles perpendicular to its plane.⁷² In 2015, Di Sante *et al.* also predicted out-of-plane ferroelectricity in 2D AB binary monolayers (e.g., GeSe and AlSb) with trigonal symmetry, where the A and B atoms belonged to groups IV or III–V.^{52,73} In these compounds, the dipoles arise from the buckled structure, where the A and B ions are located on the sites of a bipartite corrugated honeycomb lattice. Similar out-of-plane ferroelectricity existed in many other 2D materials^{74–76} such as In_2Se_3 , III₂–VI₃ compounds, phosphorene oxides, CrN, CrB_2 , and MXenes (Sc_2CO_2). A branch of 2D families based on In_2Se_3 and other III₂–VI₃ vdW materials has exhibited room-temperature ferroelectricity with reversible spontaneous electric polarization in both out-of-plane and in-plane orientations.⁷⁴ Interestingly, multiferroic properties were also found in 2D CrN and CrB_2 ; 2D CrN is found to be a 2D hyperferroelectric metal and ferromagnetic-ferroelectric multiferroic with a high critical temperature (T_C), while CrB_2 is a 2D asymmetric multiferroic suitable for realizing electric field control of magnetism.⁷⁵ Recent first-principles calculations also predicted the possible existence of ferroelectricity in the AB stacking graphitic bilayers of BN, AlN, ZnO, etc.⁷⁷

The first experimental realization for 2D ferroelectricity was in layered CuInP_2S_6 . In 2015, Belianinov *et al.* reported the observation of room-temperature out-of-plane ferroelectricity in bulk CuInP_2S_6 for film thicknesses greater than 100 nm.⁷⁸ This finding also inspired further exploration of 2D ferroelectrics in the atomically thin form. In 2016, Liu *et al.* confirmed the out-of-plane polarization in few-layer CuInP_2S_6 .⁷⁹ Using piezoresponse force microscopy (PFM) and second-harmonic generation (SHG), they observed the ferroelectric phase transition at 320 K. In 2016, Chang *et al.* experimentally reported the first 2D ferroelectric with single atomic layer thickness in monolayer SnTe. They studied the monolayer SnTe with a distorted lattice at cryogenic temperature and verified the in-plane ferroelectricity with spontaneous domains and electric polarization.⁸⁰ Recently, intrinsic room-temperature 2D ferroelectricity with a thickness down to the 2D limit was also observed in 3 nm α - In_2Se_3 (~ 3 layers),^{81–84} 1.4 nm WTe_2 (2 layers),⁸⁵ 1.2 nm α - In_2Se_3 (1–2 layers),⁸⁶ and 0.6 nm 1T MoTe_2 (1 layer).⁸⁷ These findings open up a route toward 2D ferroelectricity with a thickness down to the 2D limit.

The existence of 2D ferroelectricity was also confirmed in perovskites. So far, perovskite oxides (such as BaTiO_3 , PbTiO_3 ,

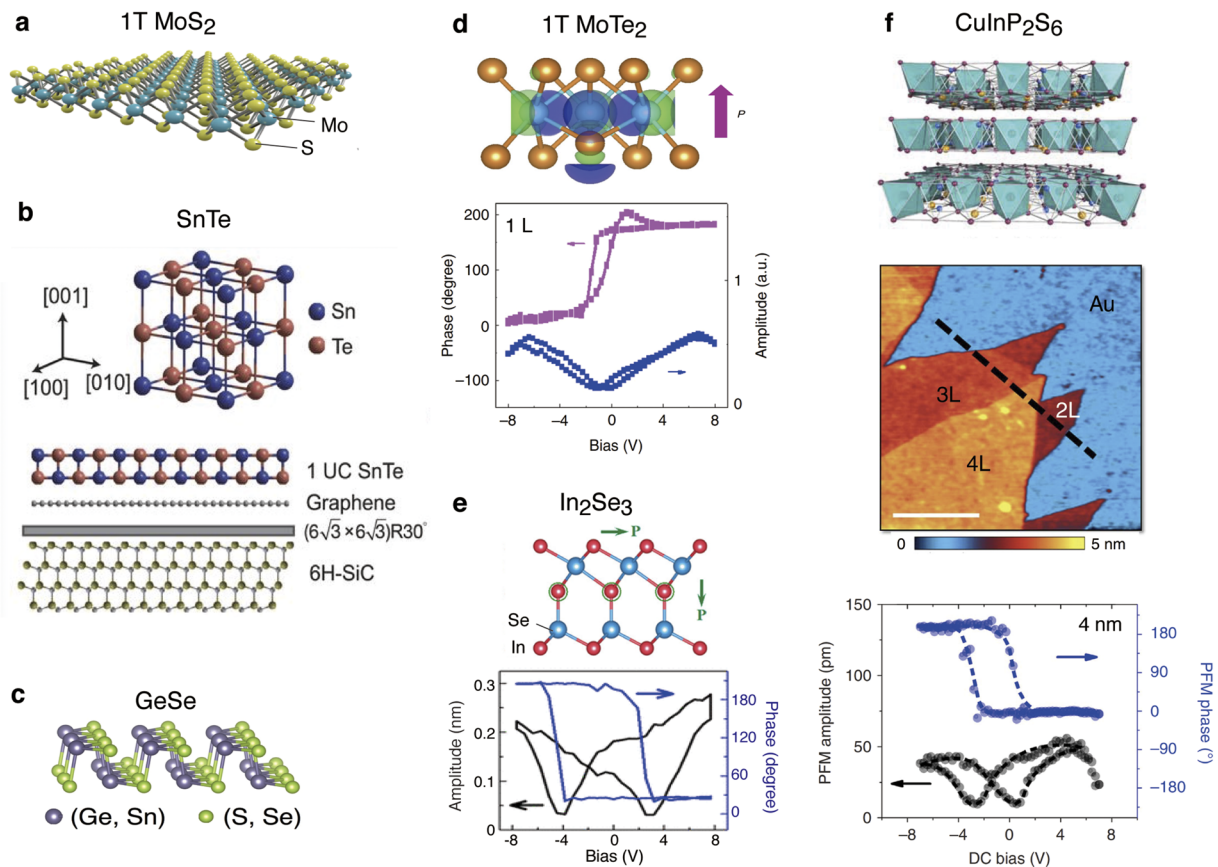


FIG. 6. Library of 2D ferroelectrics: (a) 1T MoS₂; (b) SnTe, the first 2D ferroelectric with single atomic layer thickness; (c) GeSe; (d) 1T MoTe₂, showing room-temperature 2D ferroelectricity even in monolayer (0.6 nm), (e) In₂Se₃, and (f) CuInP₂S₆. Reproduced with permission from Chang *et al.*, *Science* **353**, 274 (2016). Copyright 2016 AAAS; Yuan *et al.*, *Nat. Commun.* **10**, 1775 (2019). Copyright 2016 Springer Nature; Cui *et al.*, *Nano Lett* **18**, 1253 (2018). Copyright 2017 American Chemical Society; and Liu *et al.*, *Nat. Commun.* **7**, 12357 (2016). Copyright 2016 Springer Nature.

SrBi₂Ta₂O₉, and Bi₄Ti₃O₁₂) have been a central target for ferroelectricity in a bulk 3D system.^{14–16} Typically, d^0 cations (Ti⁴⁺, Nb⁵⁺, and Ta⁵⁺) in BO₆ octahedral units exhibit an asymmetric second-order Jahn-Teller distortion, causing a spontaneous polarization. Recently, we investigated ferroelectric properties in 2D homologous perovskite nanosheets (Ca₂Na_{m-3}Nb_mO_{3m+1}; $m = 3-6$) by using PFM and density functional theory (DFT) calculations (Fig. 7).⁴⁹ From Berry-phase calculations and soft-mode spectroscopy, we found that perovskite layer stacking (m) promoted local ferroelectric instability and that large distortions were observed in Ca₂Na₂Nb₅O₁₆, where off-center displacements of Nb⁵⁺ ions would be expected due to cooperative NbO₆ octahedral tilting with disordering at the A site. From PFM, we confirmed room-temperature out-of-plane ferroelectricity in Ca₂Na₂Nb₅O₁₆ with a thickness of 2.7 nm. More recently, Ji *et al.* demonstrated the realization of monolayer freestanding ferroelectric perovskite oxides.⁸⁸ They synthesized freestanding SrTiO₃ and BiFeO₃ ultrathin films by molecular beam epitaxy and transfer them to various substrates. Freestanding BiFeO₃ films exhibited giant tetragonality and polarization even in three-unit-cell thick. Although there were still limited numbers of reports

on 2D ferroelectricity in perovskites, these works provide a key for a long-standing conundrum of the size effect in perovskites.

IV. APPLICATIONS OF 2D DIELECTRICS/FERROELECTRICS

The unique features of 2D dielectrics/ferroelectrics make them important and fascinating research targets for device applications (Fig. 8). An important aspect of 2D nanosheets is that various nanoarchitectures can be fabricated using LEGO-like building blocks.^{6,29} By applying layer-by-layer assembly, 2D nanosheets can be organized into highly organized lamellar nanostructures and superlattices. This LEGO-like construction of 2D nanosheets opens up new avenues for creating new artificial materials and fusion devices. Furthermore, owing to the benefit of preparing stable atomically thin films, 2D nanosheets present a tantalizing prospect of scaling all electronic technology down to a truly atomic scale.

For 2D dielectrics, an important target is the development of dielectric capacitors that are the largest components in current electronic devices [Fig. 8(a)].^{6,89} For future capacitor devices, there is

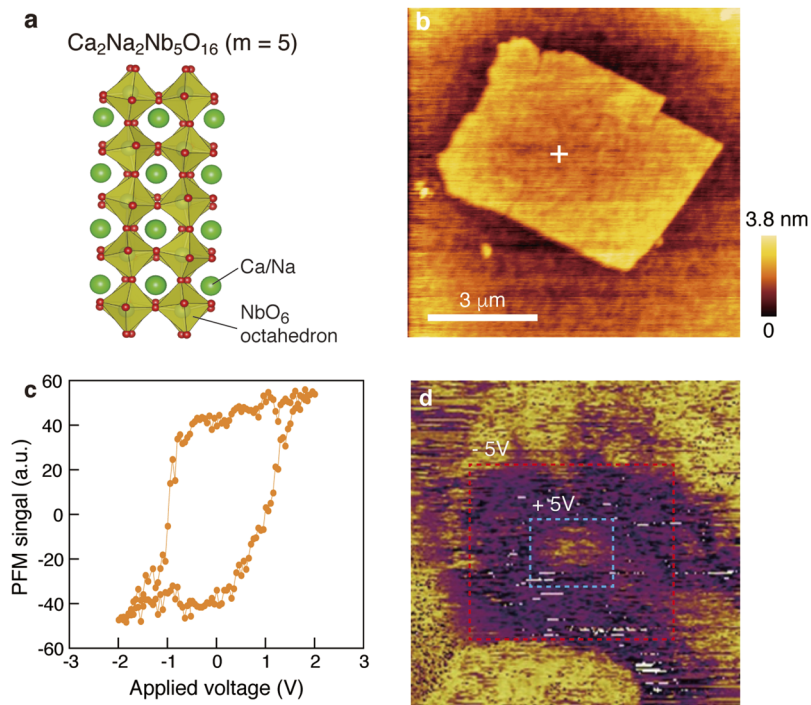


FIG. 7. 2D ferroelectric perovskite: (a) crystal structure of $\text{Ca}_2\text{Na}_2\text{Nb}_5\text{O}_{16}$ nanosheet, (b) AFM image and (c) PFM signal from $\text{Ca}_2\text{Na}_2\text{Nb}_5\text{O}_{16}$ nanosheet, and (d) PFM phase image of $\text{Ca}_2\text{Na}_2\text{Nb}_5\text{O}_{16}$ nanosheet. Reproduced with permission from Li *et al.*, *J. Am. Chem. Soc.* **139**, 10868 (2017). Copyright 2017 American Chemical Society.

a strong need to explore miniaturized dielectrics with increased ϵ_r , decreased $\tan\delta$, and reduced leakage current. It is also crucial that the capacitor components exhibit constant fidelity over wide ranges of operating conditions such as frequency and temperature (preferably up to 150 °C). 2D oxide nanosheets can satisfy these demands. Ti- or Nb-based oxide nanosheets realized excellent high- k performance ($\epsilon_r = 100\text{--}470$) even at a thickness of only a few nanometers. Because the areal capacitance (C) is governed by $C = \epsilon_0\epsilon_r/d$, where ϵ_0 and d are the vacuum permittivity and thickness, respectively, 2D oxide nanosheets provide a large capacitance density based on high ϵ_r values and molecular thicknesses. In this context, we developed high-performance all-nanosheet capacitors by sandwiching alternating metallic RuO_2 and dielectric $\text{Ca}_2\text{Nb}_3\text{O}_{10}$ nanosheets ($\epsilon_r = \sim 210$).⁹⁰ Manufactured all-nanosheet capacitors exceeded the performance of current multilayer ceramic condensers (MLCCs), opening a route to new capacitor and energy storage devices. This component is the smallest with a total thickness of ~ 30 nm and exhibited a high capacitance density ($>30 \mu\text{F}/\text{cm}^2$) and good thermal stability (up to 250 °C).⁹¹ This is just a prototype capacitor equivalent to one unit of the metal-insulator-metal structure of MLCCs, and the multilayer implementation is still challenging.

2D oxide nanosheets are a fascinating target for high-temperature applications.^{69,70,92} The development of high-temperature electronics has been a significant challenge in recent years. For example, the automotive industry requires electronic components that are operable at high temperatures (>200 °C). Most of 2D oxide nanosheets [$\text{Ti}_{0.87}\text{O}_2$, Ti_2NbO_7 , and $(\text{Ca},\text{Sr})_2\text{Nb}_3\text{O}_{10}$] are paraelectric, thus yielding a very small temperature coefficient (τ), in contrast to the large variation of ferroelectric materials.^{47,48} Another important aspect is their thermal stability.⁶⁹ In 2D nanosheets,

the crystallization and nucleation are severely hindered even at high temperatures (>800 °C). For instance, 2D oxide nanosheets [$\text{Ti}_{0.87}\text{O}_2$ and $(\text{Ca},\text{Sr})_2\text{Nb}_3\text{O}_{10}$] showed a high thermal stability up to 700 °C in a monolayer film with an extremely small thickness of ~ 2 nm. Simultaneous improvements in the dielectric constant (ϵ_r) and thermal stability are desirable for future applications, and 2D oxide nanosheets have great potential for the rational design of high-temperature capacitors and energy storage devices.

Owing to their atomically thin and flat nature, high- k nanosheets may also be used as gate dielectrics.^{6,93} In this context, hexagonal boron nitride ($h\text{-BN}$) nanosheets have been highlighted for dielectric applications.^{29,94} Unlike graphene, $h\text{-BN}$ nanosheets are an electrical insulator with a bandgap of ~ 5.8 eV.⁹⁵ $h\text{-BN}$ nanosheets also possess superb chemical and thermal stability, excellent mechanical properties, and high thermal conductivity. Due to these unique features, $h\text{-BN}$ is suitable for insulating substrates, gate dielectric layers, and tunnel barrier layers. Now, $h\text{-BN}$ is becoming a standard substrate for graphene and 2D vdW devices [Fig. 8(b)],^{29,33} where an ultraflat nature reduces charge fluctuations and thus enhances electron/hole mobility as compared with those of SiO_2 , which could improve the device performance.

Ferroelectric materials have been widely used for a range of technological applications, such as nonvolatile memories, FETs, sensors, and energy harvesting devices. Compared with that of conventional ferroelectrics in bulk and thin-film forms, 2D ferroelectrics have various advantages, such as high capacitance density, low voltage operation, flexibility, and bandgap tenability, along with promising applications as memories, FETs, and sensors. For memory devices,³⁶ 2D nanosheets would enable high capacitance density (higher density data storage) with low voltage operation (low

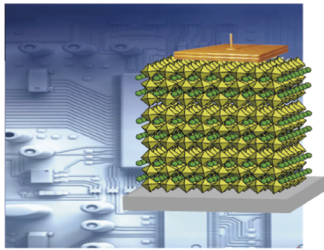
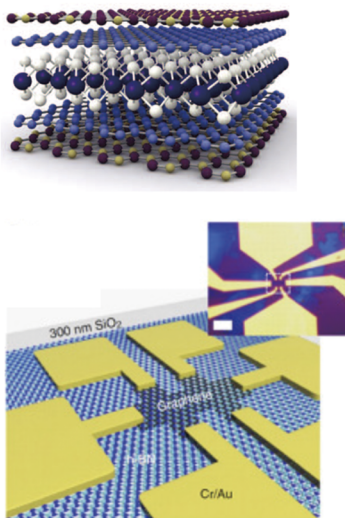
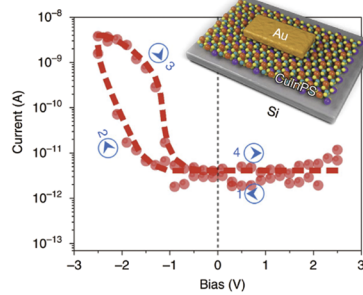
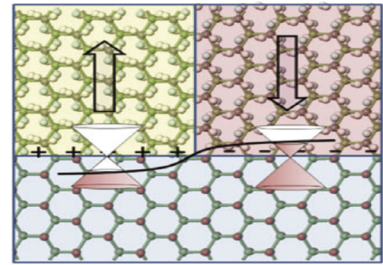
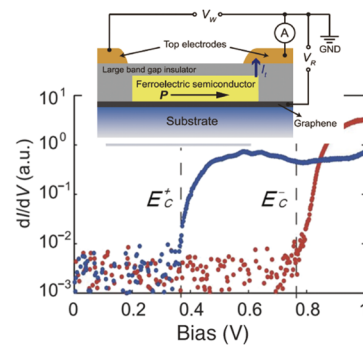
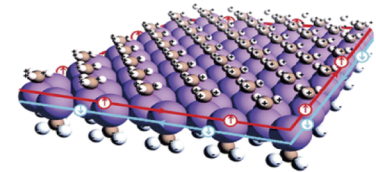
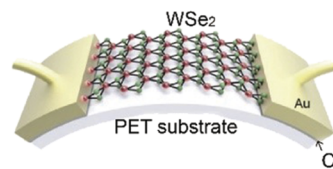
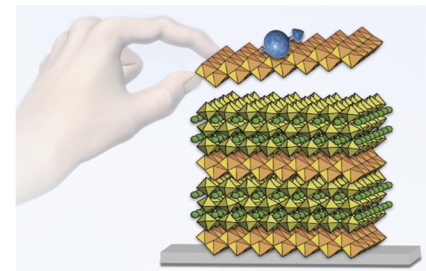
a High- k nanocapacitor**b** Super flat dielectric for vdW heterostructures**c** Ferroelectric diode**f** Ferroelectric topological transistor**d** Ferroelectric memory**g** Ferroelectric topological insulator**e** Nanogenerator & Sensor**h** Artificial multiferroic

FIG. 8. Applications of 2D dielectrics/ferroelectrics: (a) high- k nanocapacitor fabricated from perovskite nanosheets, (b) h -BN dielectrics for vdW devices, (c) ferroelectric diode using CuInP_2S_6 , (d) ferroelectric memory using SnTe , (e) nanogenerator based on WSe_2 , (f) ferroelectric topological transistor, (g) ferroelectric topological insulator based on bismuthene, and (h) artificial multiferroic superlattice composed of ferromagnetic $\text{Ti}_{0.8}\text{Co}_{0.2}\text{O}_2$ and dielectric $\text{Ca}_2\text{Nb}_3\text{O}_{10}$ nanosheets. Reproduced with permission from Novoselov *et al.*, *Science* **353**, 9439 (2016). Copyright 2016 AAAS; Liu *et al.*, *Nat. Commun.* **7**, 12357 (2016). Copyright 2016 Springer Nature; Chang *et al.*, *Science* **353**, 274 (2016). Copyright 2016 AAAS; Lee *et al.*, *Adv. Mater.* **29**, 1606667 (2017). Copyright 2017 Wiley-VCH Verlag GmbH & Co. KGaA, Weinheim; Wu *et al.*, *Nano Lett.* **16**, 7309 (2016). Copyright 2016 American Chemical Society; Hu *et al.*, *J. Mater. Chem. C* **7**, 9406 (2019). Copyright 2019 RSC; and Li *et al.*, *J. Am. Chem. Soc.* **138**, 7621 (2016). Copyright 2016 American Chemical Society.

energy consumption) relying on a high ϵ_r value and atomic thickness. 2D ferroelectric nanosheets may also realize both efficient charge injection and mobility enhancement by dielectric screening, from which we can explore high-performance FETs. Such possibilities have recently been demonstrated in some vdW materials with a small bandgap, which is desirable for high mobility and high on/off ratio transistors. In bismuth oxychalcogenides (such as $\text{Bi}_2\text{O}_2\text{S}$, $\text{Bi}_2\text{O}_2\text{Se}$, and $\text{Bi}_2\text{O}_2\text{Te}$), for example, conducting properties can be controlled by changing their ferroelectric dipolar structure with a gate voltage, providing the possibility of dipole engineering nanodevices.⁹⁷ 2D ferroelectric FETs can induce the metal–insulator transition and other novel electronic phases, which may enable a variety of applications, such as chemical sensors and catalytic structures.

In addition to these applications, practical devices based on 2D ferroelectric were also demonstrated, including switchable ferroelectric diodes, ferroelectric semiconductor FETs, and nanogenerators [Figs. 8(c)–8(e)].^{79,80,98,99} Furthermore, ferroelectric switching allows the control of asymmetry-induced properties such as spin-orbit coupling, valley degree of freedom, memristors, and anisotropic transport [Figs. 8(f) and 8(g)].^{51,100–103}

The LEGO-like construction of 2D nanosheets opens up new approaches for creating new artificial materials and fusion devices by promoting interface engineering and cooperative interactions. An interesting strategy is layering noncentrosymmetric materials in a targeted manner that lifts inversion symmetry. In current studies, the main focus has centered on the state-of-the-art layer-by-layer

growth of superlattices.^{104,105} The nanosheet approach might provide new possibilities for designing polar behavior while retaining other electronic, magnetic, or optical functionalities found in the constituent materials, thus enabling new multiferroics or polar metals [Fig. 8(h)].¹⁰⁶ Such chemical protocols using 2D nanosheets open up new pathways to create new artificial ferroelectrics/multiferroics and all-nanosheet devices.

V. SUMMARY

We have reviewed recent progress in high- k dielectric/ferroelectric properties in 2D materials. 2D nanosheets with high polarizability or noncentrosymmetric structures have great potential for high- k dielectrics/ferroelectrics. In particular, 2D oxides possess a wide bandgap (3–4 eV), which is favorable for realizing high- k dielectrics with a highly insulating nature. Newly developed high- k nanosheets ($\text{Ti}_{0.87}\text{O}_2$, Ti_2NbO_7 , $\text{Ca}_2\text{Na}_{m-3}\text{Nb}_m\text{O}_{3m+1}$) exhibited the highest permittivity ($\epsilon_r > 100$) ever realized in all known dielectrics in the ultrathin region (<10 nm).

The existence of 2D ferroelectricity was theoretically predicted a long time ago. However, there were limited numbers of reports on 2D ferroelectricity until 2014 since practical materials suffer from the fundamental constraint of size effects. In recent years, a range of 2D materials have been theoretically predicted or experimentally confirmed as ferroelectrics, those including transition metal dichalcogenides, group IV or group III–V compounds, MXenes, CuInP_2S_6 , and perovskite oxides. An important aspect is that 2D nanosheets could provide a pathway to realize 2D ferroelectricity while eliminating the so-called size-effect issues. Recently, intrinsic room-temperature 2D ferroelectricity was even observed in a monolayer of SnTe and 1T MoTe_2 with atomic-layer thickness.

The recent blossoming of high- k dielectric/ferroelectric nanosheets also provides evidence of their potential technological impact on 2D electronic devices. The addition of dielectric/ferroelectric functions to the 2D family opens up possibilities for numerous novel applications, including capacitors, sensors, actuators, nonvolatile memory devices, and various heterostructures based on 2D dielectrics/ferroelectrics. To promote such applications, we need methods for quantitative characterization of 2D dielectrics/ferroelectrics, i.e., the exact ϵ_r and polarization values in individual nanosheets along with the critical temperature (T_C) and domain structures. Compared to the long history of conventional high- k dielectrics/ferroelectrics, the research on 2D high- k dielectrics/ferroelectrics is just kicking off. We are at the starting point of learning how to utilize 2D dielectrics/ferroelectrics. Once mastered, 2D dielectrics/ferroelectrics should provide a vast and unforeseen range of science and technologies for decades to come.

ACKNOWLEDGMENTS

The authors are grateful to Dr. Y. Ebina, Dr. R. Ma, Dr. T. C. Ozawa, Dr. B.-W. Li, Dr. K. Akatsuka, Dr. H.-J. Kim, Dr. Y.-H. Kim (NIMS), and Professor K. Ono (KEK) for their experimental contributions and stimulating discussions over the years of the authors' research on 2D nanosheets. This work was in part supported by World Premier International Research Center Initiative (WPI Initiative on Materials Nanoarchitectonics), MEXT, the Grant-in-Aid for Scientific research KAKENHI, JSPS, Creation of Life Innovation

Materials for Interdisciplinary and International Researcher Development Satellite, MEXT, and the joint usage/research program of the Institute of Materials and Systems for Sustainability (IMaSS), Nagoya University.

REFERENCES

- A. I. Kingon, J. P. Maria, and S. K. Streiffer, *Nature* **406**, 1032 (2000).
- R. K. Vasudevan, N. Balke, P. Maksymovych, S. Jesse, and S. V. Kalinin, *Appl. Phys. Rev.* **4**, 021302 (2017).
- C. H. Ahn, K. M. Rabe, and J. M. Triscone, *Science* **303**, 488 (2004).
- M. Stengel and N. A. Spaldin, *Nature* **443**, 679 (2006).
- M. Stengel, D. Vanderbilt, and N. A. Spaldin, *Nat. Mater.* **8**, 392 (2009).
- M. Osada and T. Sasaki, *Adv. Mater.* **24**, 210 (2012).
- T. M. Shaw, S. Trolier-McKinstry, and P. C. McIntyre, *Annu. Rev. Mater. Sci.* **30**, 263 (2000).
- C. S. Hwang, *J. Appl. Phys.* **92**, 432 (2002).
- C. S. Hwang, S. O. Park, H. J. Cho, C. S. Kang, H. K. Kang, S. I. Lee, and M. Y. Lee, *Appl. Phys. Lett.* **67**, 2819 (1995).
- P. Padmini, T. R. Taylor, M. J. Lefevre, A. S. Nagra, R. A. York, and J. S. Speck, *Appl. Phys. Lett.* **75**, 3186 (1999).
- M. C. Werner, I. Banerjee, P. C. McIntyre, N. Tani, and M. Tanimura, *Appl. Phys. Lett.* **77**, 1209 (2000).
- J. Junquera and P. Ghosez, *Nature* **422**, 506 (2003).
- T. Tybell, C. H. Ahn, and J. M. Triscone, *Appl. Phys. Lett.* **75**, 856 (1999).
- L. W. Martin and A. M. Rappe, *Nat. Rev. Mater.* **2**, 16087 (2016).
- C. A. P. Dearaujo, J. D. Cuchiaro, L. D. McMillan, M. C. Scott, and J. F. Scott, *Nature* **374**, 627 (1995).
- B. H. Park, B. S. Kang, S. D. Bu, T. W. Noh, J. Lee, and W. Jo, *Nature* **401**, 682 (1999).
- L. W. Chang, M. McMillen, F. D. Morrison, J. F. Scott, and J. M. Gregg, *Appl. Phys. Lett.* **93**, 132904 (2008).
- L. W. Chang, M. Alexe, J. F. Scott, and J. M. Gregg, *Adv. Mater.* **21**, 4911 (2009).
- L. J. Sinnamon, M. M. Saad, R. M. Bowman, and J. M. Gregg, *Appl. Phys. Lett.* **81**, 703 (2002).
- K. Natori, D. Otani, and N. Sano, *Appl. Phys. Lett.* **73**, 632 (1998).
- D. G. Schlom, L.-Q. Chen, C.-B. Eom, K. M. Rabe, S. K. Streiffer, and J.-M. Triscone, *Annu. Rev. Mater. Sci.* **37**, 589 (2007).
- P. Gao, Z. Zhang, M. Li, R. Ishikawa, B. Feng, H. J. Liu, Y. L. Huang, N. Shibata, X. Ma, S. Chen, J. Zhang, K. Liu, E. G. Wang, D. Yu, L. Liao, Y. H. Chu, and Y. Ikuhara, *Nat. Commun.* **8**, 15549 (2017).
- D. D. Fong, G. B. Stephenson, S. K. Streiffer, J. A. Eastman, O. Auciello, P. H. Fuoss, and C. Thompson, *Science* **304**, 1650 (2004).
- Z. Wen, C. Li, D. Wu, A. Li, and N. Ming, *Nat. Mater.* **12**, 617 (2013).
- D. A. Tenne, P. Turner, J. D. Schmidt, M. Biegalski, Y. L. Li, L. Q. Chen, A. Soukiassian, S. Trolier-McKinstry, D. G. Schlom, X. X. Xi, D. D. Fong, P. H. Fuoss, J. A. Eastman, G. B. Stephenson, C. Thompson, and S. K. Streiffer, *Phys. Rev. Lett.* **103**, 177601 (2009).
- Y. H. Chu, T. Zhao, M. P. Cruz, Q. Zhan, P. L. Yang, L. W. Martin, M. Huijben, C. H. Yang, F. Zavaliche, H. Zheng, and R. Ramesh, *Appl. Phys. Lett.* **90**, 252906 (2007).
- K. S. Novoselov, V. I. Fal'ko, L. Colombo, P. R. Gellert, M. G. Schwab, and K. Kim, *Nature* **490**, 192 (2012).
- D. Akinwande, N. Petrone, and J. Hone, *Nat. Commun.* **5**, 5678 (2014).
- A. K. Geim and I. V. Grigorieva, *Nature* **499**(7459), 419–425 (2013).
- K. S. Novoselov, A. K. Geim, S. V. Morozov, D. Jiang, Y. Zhang, S. V. Dubonos, I. V. Grigorieva, and A. A. Firsov, *Science* **306**, 666 (2004).
- A. K. Geim, *Science* **324**, 1530 (2009).
- A. K. Geim and K. S. Novoselov, *Nat. Mater.* **6**, 183 (2007).
- K. S. Novoselov, A. Mishchenko, A. Carvalho, and A. H. Castro Neto, *Science* **353**, 9439 (2016).
- M. Chhowalla, H. S. Shin, G. Eda, L.-J. Li, K. P. Loh, and H. Zhang, *Nat. Chem.* **5**, 263 (2013).

- ³⁵S. Balendhran, S. Walia, H. Nili, J. Z. Ou, S. Zhuiykov, R. B. Kaner, S. Sriram, M. Bhaskaran, and K. Kalantar-zadeh, *Adv. Funct. Mater.* **23**, 3952 (2013).
- ³⁶R. Ma and T. Sasaki, *Adv. Mater.* **22**, 5082 (2010).
- ³⁷R. Ma and T. Sasaki, *Acc. Chem. Res.* **48**, 136 (2015).
- ³⁸M. Naguib, V. N. Mochalin, M. W. Barsoum, and Y. Gogotsi, *Adv. Mater.* **26**, 992 (2014).
- ³⁹M. Naguib, O. Mashtalir, J. Carle, V. Presser, J. Lu, L. Hultman, Y. Gogotsi, and M. W. Barsoum, *ACS Nano* **6**, 1322 (2012).
- ⁴⁰H. O. Churchill and P. Jarillo-Herrero, *Nat. Nanotechnol.* **9**, 330 (2014).
- ⁴¹L. Li, Y. Yu, G. J. Ye, Q. Ge, X. Ou, H. Wu, D. Feng, X. H. Chen, and Y. Zhang, *Nat. Nanotechnol.* **9**, 372 (2014).
- ⁴²Y. Saito, T. Nojima, and Y. Iwasa, *Nat. Rev. Mater.* **2**, 16094 (2016).
- ⁴³J. R. Schaibley, H. Yu, G. Clark, P. Rivera, J. S. Ross, K. L. Seyler, W. Yao, and X. Xu, *Nat. Rev. Mater.* **1**, 16055 (2016).
- ⁴⁴M. Gibertini, M. Koperski, A. F. Morpurgo, and K. S. Novoselov, *Nat. Nanotechnol.* **14**, 408 (2019).
- ⁴⁵K. Akatsuka, G. Takanashi, Y. Ebina, M.-a. Haga, and T. Sasaki, *J. Phys. Chem. C* **116**, 12426 (2012).
- ⁴⁶M. Osada, Y. Ebina, H. Funakubo, S. Yokoyama, T. Kiguchi, K. Takada, and T. Sasaki, *Adv. Mater.* **18**, 1023 (2006).
- ⁴⁷M. Osada, G. Takanashi, B.-W. Li, K. Akatsuka, Y. Ebina, K. Ono, H. Funakubo, K. Takada, and T. Sasaki, *Adv. Funct. Mater.* **21**, 3482 (2011).
- ⁴⁸M. Osada, K. Akatsuka, Y. Ebina, H. Funakubo, K. Ono, K. Takada, and T. Sasaki, *ACS Nano* **4**, 5225 (2010).
- ⁴⁹B. W. Li, M. Osada, Y. H. Kim, Y. Ebina, K. Akatsuka, and T. Sasaki, *J. Am. Chem. Soc.* **139**, 10868 (2017).
- ⁵⁰C. Cui, F. Xue, W.-J. Hu, and L.-J. Li, *npj 2D Mater. Appl.* **2**, 18 (2018).
- ⁵¹M. Wu and P. Jena, *Wiley Interdiscip. Rev.: Comput. Mol. Sci.* **8**, e1365 (2018).
- ⁵²B. J. Kooi and B. Noheda, *Science* **353**, 221 (2016).
- ⁵³T. Sasaki and M. Watanabe, *J. Am. Chem. Soc.* **120**, 4682 (1998).
- ⁵⁴M. Osada, K. Akatsuka, Y. Ebina, Y. Kotani, K. Ono, H. Funakubo, S. Ueda, K. Kobayashi, K. Takada, and T. Sasaki, *Jpn. J. Appl. Phys., Part 1* **47**, 7556 (2008).
- ⁵⁵M. Ohwada, K. Kimoto, T. Mizoguchi, Y. Ebina, and T. Sasaki, *Sci. Rep.* **3**, 2801 (2013).
- ⁵⁶M. Osada and T. Sasaki, *Dalton Trans.* **47**, 2841 (2018).
- ⁵⁷Y. Ebina, I. Sasaki, and A. Watanabe, *Solid State Ionics* **151**, 177 (2002).
- ⁵⁸Y. Ebina, K. Akatsuka, K. Fukuda, and T. Sasaki, *Chem. Mater.* **24**, 4201 (2012).
- ⁵⁹T. C. Ozawa, K. Fukuda, K. Akatsuka, Y. Ebina, and T. Sasaki, *Chem. Mater.* **19**(26), 6575–6580 (2007).
- ⁶⁰S. Ida, Y. Okamoto, M. Matsuka, H. Hagiwara, and T. Ishihara, *J. Am. Chem. Soc.* **134**, 15773 (2012).
- ⁶¹J. Gopalakrishnan, *Chem. Mater.* **7**, 1265 (1995).
- ⁶²T. C. Ozawa, K. Fukuda, K. Akatsuka, Y. Ebina, T. Sasaki, K. Kurashima, and K. Kosuda, *J. Phys. Chem. C* **112**, 1312 (2008).
- ⁶³R. E. Schaak and T. E. Mallouk, *Chem. Mater.* **12**, 2513 (2000).
- ⁶⁴R. E. Schaak and T. E. Mallouk, *Chem. Mater.* **14**, 1455 (2002).
- ⁶⁵S. Ida, C. Ogata, M. Eguchi, W. J. Youngblood, T. E. Mallouk, and Y. Matsumoto, *J. Am. Chem. Soc.* **130**, 7052 (2008).
- ⁶⁶S. Ida, C. Ogata, U. Unal, K. Izawa, T. Inoue, O. Altuntasoglu, and Y. Matsumoto, *J. Am. Chem. Soc.* **129**, 8956 (2007).
- ⁶⁷J. Y. Kim, I. Chung, J. H. Choy, and G. S. Park, *Chem. Mater.* **13**, 2759 (2001).
- ⁶⁸M. Osada and T. Sasaki, *Int. J. Appl. Ceram. Technol.* **9**, 29 (2012).
- ⁶⁹B.-W. Li, M. Osada, Y. Ebina, K. Akatsuka, K. Fukuda, and T. Sasaki, *ACS Nano* **8**, 5449 (2014).
- ⁷⁰Y. H. Kim, H. J. Kim, M. Osada, B. W. Li, Y. Ebina, and T. Sasaki, *ACS Appl. Mater. Interfaces* **6**, 19510 (2014).
- ⁷¹M. S. Khan, H.-J. Kim, T. Taniguchi, Y. Ebina, T. Sasaki, and M. Osada, *Appl. Phys. Express* **10**, 091501 (2017).
- ⁷²S. N. Shirodkar and U. V. Waghmare, *Phys. Rev. Lett.* **112**, 157601 (2014).
- ⁷³D. Di Sante, A. Stroppa, P. Barone, M.-H. Whangbo, and S. Picozzi, *Phys. Rev. B* **91**, 161401 (2015).
- ⁷⁴W. Ding, J. Zhu, Z. Wang, Y. Gao, D. Xiao, Y. Gu, Z. Zhang, and W. Zhu, *Nat. Commun.* **8**, 14956 (2017).
- ⁷⁵W. Luo, K. Xu, and H. Xiang, *Phys. Rev. B* **96**, 235415 (2017).
- ⁷⁶A. Chandrasekaran, A. Mishra, and A. K. Singh, *Nano Lett.* **17**, 3290 (2017).
- ⁷⁷L. Li and M. Wu, *ACS Nano* **11**, 6382 (2017).
- ⁷⁸A. Belianinov, Q. He, A. Dziazgys, P. Maksymovych, E. Eliseev, A. Borisevich, A. Morozovska, J. Baniys, Y. Vysochanskii, and S. V. Kalinin, *Nano Lett.* **15**, 3808 (2015).
- ⁷⁹F. Liu, L. You, K. L. Seyler, X. Li, P. Yu, J. Lin, X. Wang, J. Zhou, H. Wang, H. He, S. T. Pantelides, W. Zhou, P. Sharma, X. Xu, P. M. Ajayan, J. Wang, and Z. Liu, *Nat. Commun.* **7**, 12357 (2016).
- ⁸⁰K. Chang, J. Liu, H. Lin, N. Wang, K. Zhao, A. Zhang, F. Jin, Y. Zhong, X. Hu, W. Duan, Q. Zhang, L. Fu, Q.-K. Xue, X. Chen, and S.-H. Ji, *Science* **353**, 274 (2016).
- ⁸¹Y. Zhou, D. Wu, Y. Zhu, Y. Cho, Q. He, X. Yang, K. Herrera, Z. Chu, Y. Han, M. C. Downer, H. Peng, and K. Lai, *Nano Lett.* **17**, 5508 (2017).
- ⁸²J. Xiao, H. Zhu, Y. Wang, W. Feng, Y. Hu, A. Dasgupta, Y. Han, Y. Wang, D. A. Muller, L. W. Martin, P. Hu, and X. Zhang, *Phys. Rev. Lett.* **120**, 227601 (2018).
- ⁸³C. Zheng, L. Yu, L. Zhu, J. L. Collins, D. Kim, Y. Lou, C. Xu, M. Li, Z. Wei, Y. Zhang, M. T. Edmonds, S. Li, J. Seidel, Y. Zhu, J. Z. Liu, W.-X. Tang, and M. S. Fuhrer, *Sci. Adv.* **4**, eaar7720 (2018).
- ⁸⁴C. Cui, W. J. Hu, X. Yan, C. Addiego, W. Gao, Y. Wang, Z. Wang, L. Li, Y. Cheng, P. Li, X. Zhang, H. N. Alshareef, T. Wu, W. Zhu, X. Pan, and L. J. Li, *Nano Lett.* **18**, 1253 (2018).
- ⁸⁵Z. Fei, W. Zhao, T. A. Palomaki, B. Sun, M. K. Miller, Z. Zhao, J. Yan, X. Xu, and D. H. Cobden, *Nature* **560**, 336 (2018).
- ⁸⁶F. Xue, W. Hu, K. C. Lee, L. S. Lu, J. Zhang, H. L. Tang, A. Han, W. T. Hsu, S. Tu, W. H. Chang, C. H. Lien, J. H. He, Z. Zhang, L. J. Li, and X. Zhang, *Adv. Funct. Mater.* **28**, 1803738 (2018).
- ⁸⁷S. Yuan, X. Luo, H. L. Chan, C. Xiao, Y. Dai, M. Xie, and J. Hao, *Nat. Commun.* **10**, 1775 (2019).
- ⁸⁸D. Ji, S. Cai, T. R. Paudel, H. Sun, C. Zhang, L. Han, Y. Wei, Y. Zang, M. Gu, Y. Zhang, W. Gao, H. Huyan, W. Guo, D. Wu, Z. Gu, E. Y. Tsymlal, P. Wang, Y. Nie, and X. Pan, *Nature* **570**, 87 (2019).
- ⁸⁹H.-J. Kim, M. Osada, and T. Sasaki, *Jpn. J. Appl. Phys., Part 1* **55**, 1102A3 (2016).
- ⁹⁰C. Wang, M. Osada, Y. Ebina, B.-W. Li, K. Akatsuka, K. Fukuda, W. Sugimoto, R. Ma, and T. Sasaki, *ACS Nano* **8**, 2658 (2014).
- ⁹¹M. S. Khan, M. Osada, H.-J. Kim, Y. Ebina, W. Sugimoto, and T. Sasaki, *Jpn. J. Appl. Phys., Part 1* **56**, 06GH09 (2017).
- ⁹²Y.-H. Kim, M. Osada, L. Dong, H.-J. Kim, and T. Sasaki, *J. Ceram. Soc. Jpn.* **123**, 335 (2015).
- ⁹³M. Osada and T. Sasaki, *J. Mater. Chem.* **19**, 2503 (2009).
- ⁹⁴C. R. Dean, A. F. Young, I. Meric, C. Lee, L. Wang, S. Sorgenfrei, K. Watanabe, T. Taniguchi, P. Kim, K. L. Shepard, and J. Hone, *Nat. Nanotechnol.* **5**, 722 (2010).
- ⁹⁵K. Watanabe, T. Taniguchi, and H. Kanda, *Nat. Mater.* **3**, 404 (2004).
- ⁹⁶S. Wan, Y. Li, W. Li, X. Mao, C. Wang, C. Chen, J. Dong, A. Nie, J. Xiang, Z. Liu, W. Zhu, and H. Zeng, *Adv. Funct. Mater.* **29**, 1808606 (2019).
- ⁹⁷M. Wu and X. C. Zeng, *Nano Lett.* **17**, 6309 (2017).
- ⁹⁸J. H. Lee, J. Y. Park, E. B. Cho, T. Y. Kim, S. A. Han, T. H. Kim, Y. Liu, S. K. Kim, C. J. Roh, H. J. Yoon, H. Ryu, W. Seung, J. S. Lee, J. Lee, and S. W. Kim, *Adv. Mater.* **29**, 1606667 (2017).
- ⁹⁹S. Wan, Y. Li, W. Li, X. Mao, W. Zhu, and H. Zeng, *Nanoscale* **10**, 14885 (2018).
- ¹⁰⁰M. Wu, S. Dong, K. Yao, J. Liu, and X. C. Zeng, *Nano Lett.* **16**, 7309 (2016).
- ¹⁰¹K. Chang, B. J. Miller, H. Yang, H. Lin, S. S. P. Parkin, S. Barraza-Lopez, Q.-K. Xue, X. Chen, and S.-H. Ji, *Phys. Rev. Lett.* **122**, 206402 (2019).
- ¹⁰²X.-K. Hu, Z.-X. Pang, C.-W. Zhang, P.-J. Wang, P. Li, and W.-X. Ji, *J. Mater. Chem. C* **7**, 9406 (2019).
- ¹⁰³F. Xue, X. He, J. R. D. Retamal, A. Han, J. Zhang, Z. Liu, J. K. Huang, W. Hu, V. Tung, J. H. He, L. J. Li, and X. Zhang, *Adv. Mater.* **31**, 1901300 (2019).
- ¹⁰⁴B.-W. Li, M. Osada, T. C. Ozawa, Y. Ebina, K. Akatsuka, R. Ma, H. Funakubo, and T. Sasaki, *ACS Nano* **4**, 6673 (2010).
- ¹⁰⁵Y.-H. Kim, L. Dong, M. Osada, B.-W. Li, Y. Ebina, and T. Sasaki, *Nanotechnology* **26**, 244001 (2015).
- ¹⁰⁶B.-W. Li, M. Osada, Y. Ebina, S. Ueda, and T. Sasaki, *J. Am. Chem. Soc.* **138**, 7621 (2016).